

Geometrical characterization of ship structural design

R. Machado, J.M. Gordo & M. Ventura

Centre for Marine Technology and Ocean Engineering (CENTEC), Instituto Superior Técnico, Universidade de Lisboa, Lisbon, Portugal

ABSTRACT: This work aims to achieve two goals: to gather a set of data consisting of the geometric characterization of several ships, at both a global and local level and to study how these geometrical characteristics affect some of the most important structural design aspects, namely the stiffened panel strength, the local strength assessment of the secondary structure and the total panel production costs. For this purpose, two databases were implemented: ships database presenting all the global geometrical characteristics of several ships; ship panels database, which comprised all the geometrical information at a local level. Three main studies were carried out focusing on structural integrity and production costs. The stiffened panel strength study and the local strength assessment allow evaluating the structural integrity of the ship was affected by variables. The panel production costs assessment evaluates how ship types and their dimensions affect the profitability of a newbuilding.

1 INTRODUCTION

In recent years, most sectors of society have seen their activities impacted or completely changed with the usage of data analytics – the practice of using data to manage information and performance. This trend is no longer limited to top-end companies, as 59% of enterprises are using Big Data Analytics (BDA) to make better decisions, enable key strategic initiatives and to improve relationships with both customers and business partners (Columbus, 2018). The maritime sector itself has experienced a shift in paradigm that led to the implementation of BDA in multiple areas. Whether due to the legislation regarding emissions, the need to become more efficient in an increasingly competitive shipbuilding market, the need to optimize existent and new routes for more viable shipping or simply to ensure more safe sailing, the maritime industry has really pushed to stay up to par with other sectors.

The present thesis aims to create a database consisting of both the general characteristics of ships and the geometrical characteristic of the corresponding midship sections. The mentioned database can then be used to assess the influence of several global (ship geometry) or local (panel geometry) level parameters on several aspects, ranging from the ship's structural integrity to its building costs. One of the main objectives of this thesis is to evaluate how the geometrical characteristics of ship structures influence the ship panel strength, to establish further relations regarding how the panel strength is influenced by the considered panel type, ship type or ship length. Correspondingly, a local strength assessment of secondary structure will also be implemented with respect to the

gathered data. Additionally, a similar evaluation will be carried out regarding the overall production costs of ship panels, and the way how these are affected by the considered panel type or ship type.

2 BACKGROUND

Firstly, a brief review of previously established methods that led to the most up to date formulations for the estimation of stiffened panels strength will be made.

Afterwards, the evaluation of the bending stress of the secondary structure will be introduced, with an explanation of how this assessment differs from the stiffened panel strength dealt with previously. Besides, the impact of ship length on the importance of this aspect in comparison with stiffened panels strength will be addressed.

Lastly, a short overview of developments in the shipbuilding industry will be presented.

2.1 *Methods for the estimation of stiffened panels strength*

The behaviour of stiffened plates under predominantly compressive loads is significantly difficult to describe due to the number of possible combinations of plate and stiffener geometry, boundary conditions and loads applied. Nevertheless, and to minimize the computer power and time consumption associated with finite element modelling, simplified formulations have been frequently used for both strength assessment and design purposes.

Several attempts to capture how a stiffened panel contributes to the overall strength of the hull girder have been made since the 1960's. Caldwell (1965) and later Faulkner (1975) worked on a method to calculate the ultimate moment of a midship section, considering an instability strength reduction factor for compressed structures. An engineering approach was considered by Billingsley (1980), when each beam-column element was modelled individually, with the strength of the hull girder being obtained from the summation of each contribution. These approaches based their predictions on the collapse strength of an individual plate, while subsequent methods such as Adamchak (1984) and Lin (1985) considered the sequence of collapsing plates.

Significant results were drawn by Rutherford & Caldwell (1990), when analysing a specific case study where a Very Large Crude Carrier broke. The comparison between the ultimate bending moment experienced by the vessel under analysis and the theoretical predictions of the ultimate longitudinal bending strength of the hull considering a simplified, approach allowed to validate the considered model.

The method proposed by Gordo & Guedes Soares (1993) consisted in the production of load shortening curves for stiffened plates based on mathematical expressions which had been proved to be appropriate for design purposes. This method assumes that the considered materials present an elastic-perfectly plastic behaviour. This approximation is accurate for most structural steels, as the strains attained until collapse will never surpass three or four times the yield strain.

The compressive strength of a plate depends on its geometry and mechanical properties, namely on its slenderness - β - which translates the geometrical relation between the plate's width, thickness, Young's modulus and yield strain.

A typical approach to deal with the reduced strength of the plates is by equating it to the strength of a plate with an effective width Φ_w , that collapses at nominal yield stress.

Faulkner *et al.*(1973) established a model based on the Johnson-Ostenfeld formulation for the ultimate strength of thin stiffened plates where both the stiffener and an effective strip of the plate are subjected to an edge stress.

The average stress of a column under its yield strain, consists of a weighted average considering both stiffener and plate area contributions (considering effective plate width) to the column stress. Since this average stress is evaluated at yield strain, it translates the compressive strength of the stiffened plate column.

2.2 Local strength assessment of secondary structure

In the present chapter, another important component of the database analysis will be introduced: the local strength assessment of secondary structure. Unlike

the previously addressed variable, the stiffened panel strength, which assessed how each panel element contributed to the overall midship section strength, this entity evaluates how stiffened panels respond under local lateral pressures

This assessment is carried out using a simple mechanics of materials approach. The stiffened panel element is modelled as a beam, simply supported on its ends (corresponding to the length between consecutive frames) and subjected to a uniformly distributed load, which represents the applied local lateral pressure. Then, and knowing the bending moment distribution, it becomes possible to assess the maximum bending stress depending on the applied lateral pressure.

For larger vessels, where the more significant loads are due to the balancing of longitudinal weight and buoyancy distributions, the stiffened panel strength is the defining design variable. On the other hand, smaller vessels are more drastically influenced by local loads, namely regarding lateral pressure. Considering this aspect, it is expected to find visible differences between the local strength assessment for smaller and larger vessels.

2.3 Shipbuilding industry overview

The international competition from Far-East shipbuilding companies, that has been experienced by the European shipbuilding industry in the last decades, has seriously influenced new ship orders. This led to studies regarding the feasibility of new technologies in the production process, namely regarding the improvement in both cutting and welding technologies, as referred by Gordo *et al.* (2006).

A study to evaluate the implementation of different cutting and welding procedures to analyse the consequences on the variation of the production's time and cost parameters was carried out by Leal & Gordo (2017). Also, by implementing and developing simulation tools, other sets of studies were conducted to obtain a better understanding of the production flow when faced with different production options (Ljubenkov *et al.*, 2008)(Oliveira & Gordo, 2018).

Many shipyards derive cost estimates based on the costs per ton or man-hours per ton, which are typically obtained from records of recent construction projects. However, there's been an increasing demand for more accurate methods. Lin and Shaw (2017) developed an innovative cost estimation method called the feature-based estimation, based on the preliminary specifications to estimate ship costs, including the steel, other main materials, engine, power generator, other core equipment and labour hours.

3 IMPLEMENTATION

This chapter will introduce the significant ships database and the ship panels database. Besides, all the

practical aspects regarding the implementation of the stiffened panel strength, local strength assessment of secondary structure and production costs formulations will be introduced, explaining all the assumptions made for a general case study.

3.1 Significant ships database

To significantly represent the shipbuilding industry worldwide, the established database comprises data collected from the midship section drawings of 15 ships built in shipyards from across the globe. For each of the entries of the significant ship database, the following data was gathered:

- Ship type
- Length between perpendiculars (LPP)
- Breadth
- Scantling draught
- Web frame spacing (l)

The gathered database presents a wide scope of vessels that depict the shipbuilding market over the last decades. With an even distribution regarding both the ship types and ship lengths (as depicted in Table 1 and Table 2, respectively), it becomes possible not only to assess global tendencies in terms of panel strength and production costs, but to extend this type of analysis to a more detailed level, focusing on trends evidenced by each individual ship type.

Table 2, respectively), it becomes possible not only to assess global tendencies in terms of panel strength and production costs, but to extend this type of analysis to a more detailed level, focusing on trends evidenced by each individual ship type.

Table 1. Significant ships database composition in ship types.

Ship type	Number of entries
Bulk carrier	3
Container carrier	2
Multipurpose vessel	3
Passenger ship	4
Tanker	3

The relation between each entry of the significant ships database and the entries of the ship panels database is described in Figure 1. For instance, if the considered significant ships database consists of n ships, and each of the ships presents m significant panels, the ship panels database will be constituted by $n \times m$ entries.

Table 2. Significant ships database composition in LPP [m].

LPP [m]	Number of entries
73 – 114	4
114 – 155	3
155 – 196	1
196 – 238	2
238 – 279	3
279 – 320	2

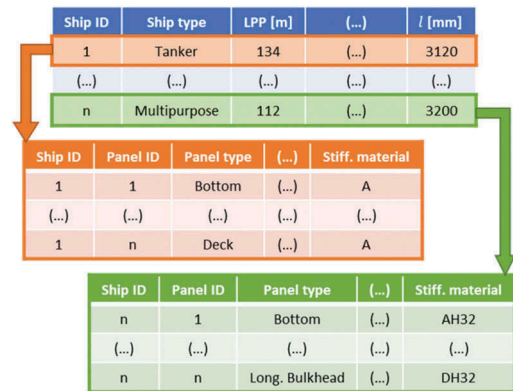


Figure 1. Integration of significant ships database and ship panels database.

3.2 Ship panels database

A subsequent database was defined to comprise all the information regarding every individual stiffened panel found in each of the entries of the significant ships database. To keep a pattern when inputting the stiffened panel data in the database, the only structural areas considered were the bottom, deck, double bottom, longitudinal bulkhead, and side shell areas. Considering the typical arrangement of a general stiffened panel, the following essential data was gathered for the ship panel database:

- Panel type
- Location (when applicable)
- Longitudinal stiffener spacing
- Plate thickness
- Plate material
- Stiffener type (flat bar, bulb, angle, or T cross-sections)
- Stiffener web height
- Stiffener flange width (when applicable)
- Stiffener web thickness
- Stiffener flange thickness (when applicable)
- Stiffener material

The composition of the ship panels database regarding the considered panel types is displayed in Table 3, showing a good representation of every type of panel.

Table 3. Ship panels database composition in panel types.

Panel type	Number of entries
Bottom	15
Deck	22
Double bottom	15
Longitudinal bulkhead	25
Side shell	30

3.3 Geometrical definition of a stiffened panel

An example of a typical stiffened panel cross-section is shown in Figure 2. The two main geometrical aspects that define the plating are the plate thickness, t_p , and the plate breadth, b . The plate breadth is defined as the transverse distance between two consecutive longitudinal stiffeners. The plating material is usually characterized by its Young's modulus, E , and yield stress, σ_0 .

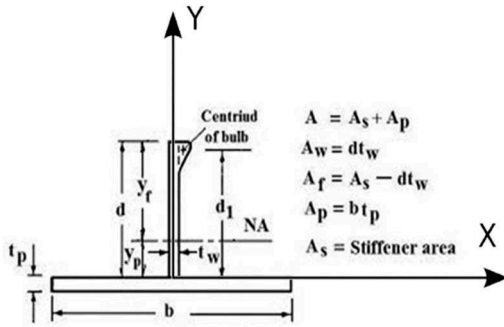


Figure 2. Geometric definition of a stiffened panel (bulb cross-section).

Stiffener types such as flat bars and bulb flats are characterized by web height, d_w , and web thickness, t_w . Angle and T cross-section stiffeners are additionally characterized by flange breadth, b_f , and flange thickness, t_f . Besides, and in the same way as the plating, the stiffener material is characterized by both Young's modulus and yield stress.

The cross-section properties of a typical stiffened panel can be derived from equations using the entities presented throughout the present chapter and considering a coordinates system in accordance with the one presented in Figure 2. The most significant

property obtained from the panel geometry is the second moment of area about the x-axis, I_{xx} , which will be necessary to evaluate the radius of gyration of the cross-section of the column.

3.4 Implementation of stiffened panel strength formulations

The present section presents the equations used to implement the method mentioned in Chapter 2.1. In accordance with what had been stated previously, the method for the computation of stiffened panel strength assumes an elastic-perfectly plastic behaviour of the considered materials.

$$\Phi(\bar{\varepsilon}) = \Phi_e = \begin{cases} -1, \bar{\varepsilon} < -1 \\ \bar{\varepsilon}, -1 < \bar{\varepsilon} < 1 \\ 1, \bar{\varepsilon} > 1 \end{cases} \quad (1)$$

In Equation (1) Φ_e is the edge stress ratio, i.e. the ratio between edge and yield stress, and $\bar{\varepsilon}$ is the average strain ratio, i.e. the ratio between edge and yield strain, ε_0 .

$$\beta = \frac{b}{t_p} \cdot \sqrt{\varepsilon_0} \quad (2)$$

Equation (2) defined the plate slenderness, β , where b is the plate breadth and t_p is the plate thickness.

$$\Phi_w = \frac{2}{\beta} - \frac{1}{\beta^2}, \beta > 1 \quad (3)$$

Equation (3) depicts how the effective width of the plate Φ_w , goes from a value close to 1 to lower values, as the loading (and consequently the strain) is increasing. The normalised average stress of the plate, Φ_a , is obtained by the product of edge stress (Equation (1)) and the corresponding effective width (Equation (3)), as shown in Equation (4).

$$\Phi_a = \Phi_e \cdot \Phi_w \quad (4)$$

Later, it becomes necessary to define the Euler stress ratio, Φ_E , using Equation (5). This ratio is defined as a function of the column slenderness, λ , which is defined in Equation (6).

$$\Phi_E = \left(\frac{\pi}{\lambda}\right)^2 \quad (5)$$

$$\lambda = \frac{l}{r} \sqrt{\varepsilon_0} \quad (6)$$

In the previous expression, r translates the radius of gyration of the cross-section of the column, which

can be evaluated using Equation (7). Here, I_{xx} is the second moment of area about the x-axis and A_s is the cross-section area of the stiffener.

$$r = \sqrt{\frac{I_{xx}}{A_s + b \cdot t_p}} \quad (7)$$

Johnson-Ostenfeld contribution for the average stress of a column, Φ_{jo} , is then evaluated using Equation (8).

$$\Phi_{jo} = \begin{cases} \Phi_E \cdot \Phi_e, & \Phi_E < 0.5 \\ \left(1 - \frac{1}{4\Phi_E}\right) \Phi_e, & \Phi_E > 0.5 \end{cases} \quad (8)$$

Finally, the expression to calculate the average stress of a column under its yield strain, ϵ_0 , and hence the compressive strength of a stiffened plate column, is obtained and presented in Equation (9).

$$\Phi_{ab} = \Phi_{jo} \cdot \frac{\frac{A_s}{b \cdot t_p} + \Phi_w}{\frac{A_s}{b \cdot t_p} + 1} \quad (9)$$

3.5 Implementation of the local strength assessment of secondary structure

In the present chapter, the implementation of the local strength assessment procedure will be explained in detail. The mechanics of materials approach used to model the panel structure will be dealt with, deducting the relevant expressions from classic formulations, and justifying the assumptions made. Besides, the significant differences between stiffened panel strength and local strength assessment and the respective expected influence on the obtained results, will be discussed.

The mechanics of materials approach is based on the analogy between a simply supported beam subjected to uniformly distributed load (Figure 3) and a stiffened panel subjected to a local lateral pressure.

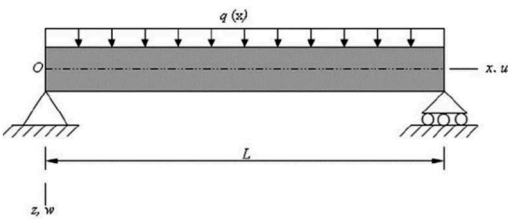


Figure 3. Simply supported beam subjected to uniformly distributed load.

Regarding the scheme presented in Figure 3, the simply supported ends of the beam can be compared to the web frame ends of a stiffened panel, hence the beam length, L , is evaluated as the length between frames, l . Besides, the uniformly distributed load q , can be represented by the product between the longitudinal stiffener spacing, s , and the local lateral pressure, p . It was considered that the web frames limiting the stiffened panels wouldn't restrict the rotation of the panels ends, hence the assumption of simply supported beam ends.

Correspondingly, it becomes possible to define an expression for the maximum bending stress, σ_{xmax} :

$$\sigma_{xmax} = \frac{M_{max} \cdot c}{I_{xx}} = \frac{p \cdot s \cdot l^2}{8} \cdot \frac{c}{I_{xx}} \quad (10)$$

Where c denotes the neutral axis position, which in this case equals the vertical centre of gravity of the beam cross section. To present results without having to assume lateral pressure values, the present study will focus on two distinct variations of the maximum bending stress expression. One will be the ratio between maximum bending stress and lateral pressure, shown in Equation (11), leading to the evaluation of the magnitude of the attained maximum bending stress for a unity of lateral pressure. The second one, shown in Equation (12), presents the lateral pressure value at which the attained maximum bending stress equals the yield stress.

$$\frac{\sigma_{xmax}}{p} = \frac{s \cdot l^2 \cdot c}{8 \cdot I_{xx}} \quad (11)$$

$$p = \frac{8 \cdot I_{xx} \cdot \sigma_0}{s \cdot l^2 \cdot c} \quad (12)$$

Significant differences are expected regarding the results for both stiffened panel strength and local strength assessment. The stiffened panel strength results translate how effective is the contribution of each of the stiffened panel elements to the overall midship section strength, which allows to assess how much of the bending moment (hog and sag) the vessel can tolerate. On the other hand, the local strength assessment using the mechanics of materials approach previously described, allows to evaluate the maximum bending stress caused by a local lateral pressure along a stiffened panel.

Considering the global (stiffened panel strength) and local (local strength assessment) character of these two approaches, it becomes logical that their relative importance to the design process is also dependent on the considered situation. For smaller sized vessels (for instance, with LPP lower than 150 m) the local approach will become more significant, while for larger vessels the global approach considering longitudinal bending will be driving the design process.

3.6 Implementation of production costs formulations

The practical aspects considered in the computations of each individual contribution to the overall production cost of a stiffened panel will be presented and discussed in the present section. For the sake of this study, material, cutting, assembly, and welding costs were considered as the defining components to the overall production costs for standard stiffened panel shipbuilding.

The material costs were considered as the simple acquisition costs for the steel plates and stiffeners. Since most of this market regards prices per unit weight of steel, the first step was to calculate the plate and stiffener weights, W_p and W_s , respectively. These depend solely on their geometry and steel density, ρ_{steel} , considered as 7.85 t/m^3 . Finally, and considering 600 €/t and 412 €/t as the plate and stiffener prices per unit weight, respectively, the total material costs, C_m , were evaluated using Equation (13).

$$C_m = 600 \cdot W_p + 412 \cdot W_s \quad (13)$$

The cutting costs regarded for this study comprise two main components: operational cutting costs and electricity costs. The operational costs are the result of a deduction made in the work of Leal and Gordo (2017), where shipyard estimated costs of 150 €/t of steel were considered. The electricity costs account for an estimated plasma cutting power of 55 kW at a price of 0.10 €/kWh. The electricity consumption can be estimated using the cutting time, which needs to be evaluated using an assumed plasma cutting speed of 99.5 m/h and the cutting length, l_c . The previously referred assumptions regarding the cutting process are included in Equation (14), which defined the total cutting costs, C_c .

$$C_c = 150 \cdot (W_p + W_s) + 0.10 \cdot 55 \cdot \frac{l_c}{99.5} \quad (14)$$

The assembly costs translate the work force required to assemble the longitudinal stiffeners in their respective welding position. Leal & Gordo (2017) estimated a work efficiency of around 0.56 man-hours per metre of longitudinal stiffener assembly, which combined with an assumed work cost of 8 € per man-hour, leads to an estimate of total assembly costs, C_a , as shown in Equation (15).

$$C_a = 8 \cdot \left(0.56 \cdot l \cdot 10^{-3} \cdot \frac{w_p}{s} \right) \quad (15)$$

The welding costs are computed based on the welding electrode consumption. To correctly estimate the consumption of the electrode, one must consider the

differences between plate-plate welds (butt joints) and plate-stiffener welds (tee joints). These differences appear in both the considered weld length and cross-section area. After correctly evaluating each of the different weld types in each of the considered panels, the corresponding total weld weight (in kg), W_w , is computed. Finally, and considering a price of 38€ for each 16 kg electrode reel, (as estimated in Leal & Gordo (2017)), the total welding costs, C_w , are calculated using Equation (16).

$$C_w = 38 \cdot \frac{W_w}{16} \quad (16)$$

4 RESULTS

The presented methods regarding panel strength assessment (Chapter 3.4), local strength assessment of secondary structure (Chapter 3.5) and production costs (Chapter 3.6) were applied to the gathered ship panel database. Afterwards, the attained results regarding panel strength, local strength assessment and production costs will be subjected to several parametric analyses.

This procedure aims at understanding how the variables under study are related to geometric characteristics at a global (ship geometry) or local (panel geometry) level. In each of the following chapters, different studies were carried out depending on the analysed feature, as certain aspects are not equally influential for either panel strength, local strength assessment or production costs due to the major disparities between what these parameters stand for.

4.1 Stiffened panel strength results

In the present chapter, the results obtained regarding panel strength will be presented in two distinct approaches: as function of LPP and as function of panel aspect ratio, α (the ratio between panel length, which corresponds to the web frame spacing, l , and panel width, w_p), defined in Equation (17).

$$\alpha = \frac{l}{w_p} \quad (17)$$

The choice of these two parameters has to do with, as previously pointed out, the attempt to establish relations between panel strength and both ship-level and panel-level variables.

Overall, the bottom panel strength results shown in Figure 4, depict a proportional increase in panel strength with LPP (as seen in the fitting line expression for multipurpose vessels in Equation (18)), until an asymptote is reached at about 0.9, for LPP values higher than 200 m.

$$\text{Panel strength} = 0.002 \times \text{LPP} + 0.326 \quad (18)$$

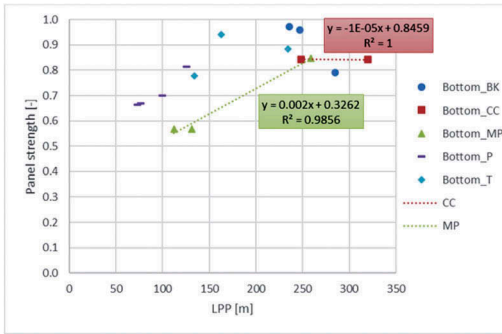


Figure 4. Bottom panel compressive strength as a function of LPP [m].

Regarding double bottom panel strength, Figure 5 shows similar tendencies when comparing to the bottom panel results presented in Figure 4, with an increase in panel strength caused by the increase in LPP.

Figure 6 Displays how deck panels also follow the overall trend of increasing panel strength with increasing LPP values. The behaviour evidenced by deck panels regarding their strength, shows much higher values for cargo vessels (namely bulk carriers and tankers) when in comparison to passenger vessels.

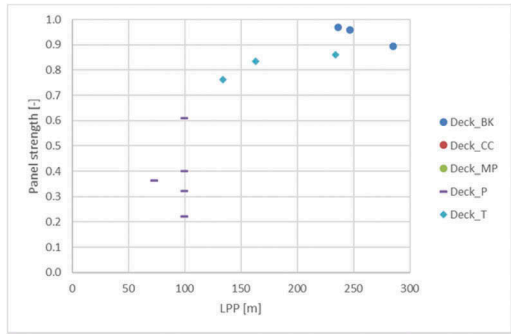


Figure 6. Deck panel compressive strength as a function of LPP [m].

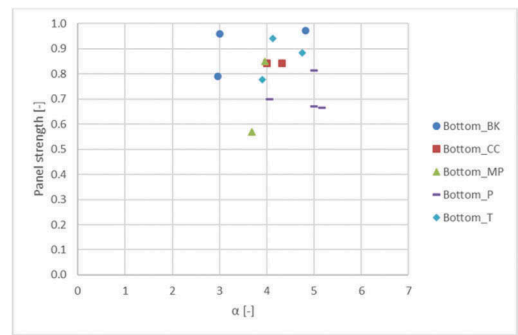


Figure 7. Bottom panel compressive strength as a function of panel aspect ratio, α .

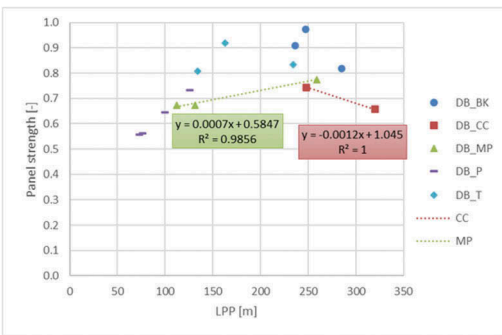


Figure 5. Double bottom panel compressive strength as a function of LPP [m].

The strength results regarding bottom panels presented in Figure 7 show how the evaluation of this variable as a function of panel aspect ratio leads to a cluster-like distribution.

Most panel strength values seem to be dispersed around a central value of 0.8, with α values ranging from 3 to 5.

4.2 Local strength assessment of secondary structure results

Similar to Section 3.5, the results of the local strength assessment of secondary structure will be presented in two distinct variations of the maximum bending stress expression shown in Equation (10). The first one, shown in Equation (11), presents the ratio between maximum bending stress and lateral pressure, leading to the evaluation of the magnitude of the attained maximum bending stress for a given lateral pressure. The second one, shown in Equation (12), presents the lateral pressure value at which the attained maximum bending stress equals the yield stress. In either case, both the influence on the results of a ship-level variable (LPP), and a panel-level variable (α) will be assessed.

Figure 8 shows the local strength results for double bottom panels as a function of LPP.

The results shown in Figure 8 for double bottom panels translate a decrease in maximum bending stress with increasingly higher LPP values. However, it must be pointed out how for these larger LPP values, the maximum bending stress tends to stabilize around a plateau.

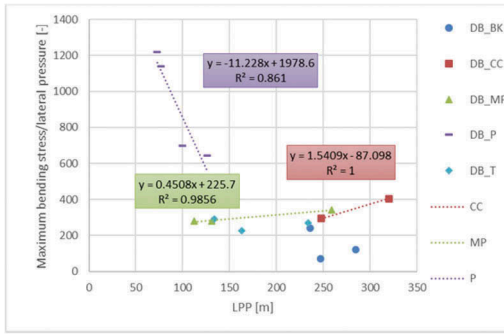


Figure 8. Maximum bending stress over lateral pressure for double bottom panels as a function of LPP [m].

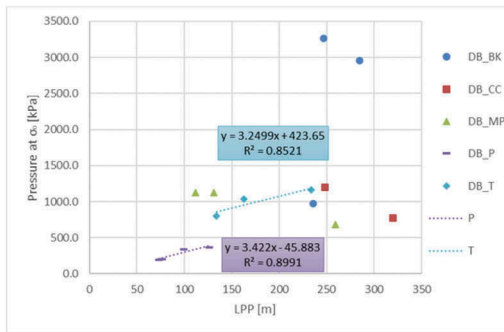


Figure 9. Pressure to reach bending yield stress for double bottom panels as a function of LPP [m].

Figure 9 presents the pressure to reach bending yield stress results for double bottom panels.

A general tendency of linear increase in pressure to reach bending yield stress with the increase in LPP is observed as expected, namely for tanker vessels (fitting line expression in Equation (19)). Considering the relation between the expressions for maximum bending stress over lateral pressure and the pressure to reach bending yield stress described in Chapter 3.5, the results are as expected.

$$Pressure\ at\ \sigma_0 = 3.25 \times LPP + 424 \quad (19)$$

The side shell panel results for maximum bending stress over lateral pressure as function of α shown in Figure 10 present linear trends within specific ship types. However, the overall behaviour for this panel type is of a cluster-like concentration around a maximum bending stress over lateral pressure ratio of 300.

The results shown in Figure 11 allow to assess a decrease in pressure to reach bending yield stress with slenderer panels (larger α values), for

side shell panels. In this case, three distinct clusters can be identified: one around 2500 kPa for α values around 3, one around 1000 kPa for α values around 4 and one around 200 kPa for α values between 5 and 7.

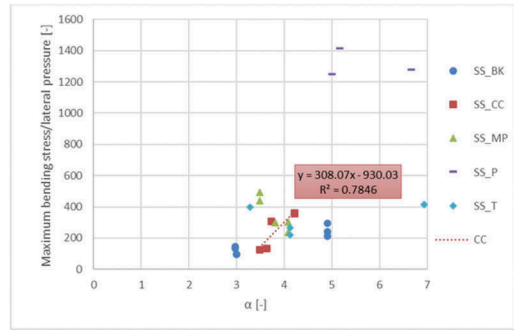


Figure 10. Maximum bending stress over lateral pressure for side shell panels as a function of panel aspect ratio, α .

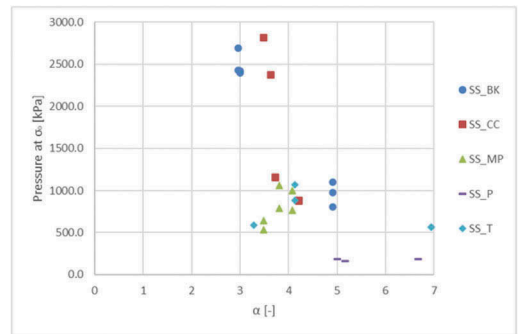


Figure 11. Pressure to reach bending yield stress for side shell panels as a function of panel aspect ratio, α .

4.3 Production costs results

In the present chapter, the production costs introduced in Chapter 3.6 will be analysed in two distinct ways: production costs per unit area (TPPCA) and production costs per unit weight (TPPCW). In the first one, the total production costs of each panel are divided by the panel's area, while on the second one the same production costs are divided by the panel's weight. Both studies will present production costs results as a function of LPP. The main objective of this distinction is to assess how differently the two main characteristics of a shipbuilding panel – its area and weight – impact the overall production costs.

A comparative study between the production costs of each panel type and the respective

bottom panel production costs was also carried out regarding both costs per unit area and weight. Using the ratio between the production cost of each considered panel and the production cost of the respective bottom panel, it becomes possible to evaluate trends with respect to a benchmark value of each of the ships in the database.

In general, Figure 12 shows how TPPCA are directly proportional to the LPP of the considered ship. For LPP values lower than 200 m, a clear linear increase in TPPCA with increase in LPP is found.

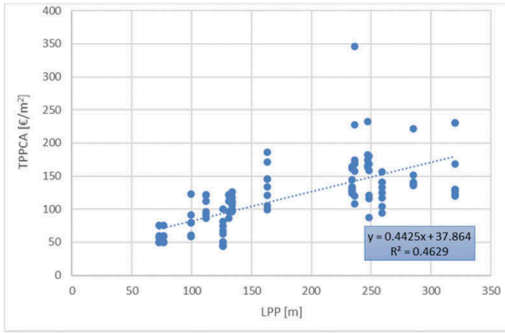


Figure 12. TPPCA [€/m²] as a function of LPP [m].

On the other hand, for LPP values higher than 200 m, the TPPCA seem to remain constant despite the increase in LPP. This is due to the ship types in each LPP range, as the lowest LPP range is associated with passenger and multipurpose vessels, while the highest LPP range is associated with tanker, bulk and container carrier vessels.

Besides, it was assessed how larger or smaller the TPPCA of each panel type are in comparison to the TPPCA of bottom panels. For this, the ratio between the TPPCA of each panel type and the TPPCA of the corresponding bottom panel (Equation (20)) is analysed as a function of LPP.

$$\frac{TPPCA_{chosen\ panel}^{ship\ n}}{TPPCA_{bottom\ panel}^{ship\ n}} \quad (20)$$

The TPPCA results for bottom panels are shown in Figure 13, presenting a global linear increase in TPPCA with increasingly higher LPP values (evident when considering the presented overall fitting line expression).

Bottom panels were defined as the benchmark for this comparison, as they are usually the stiffest panels of the midship section. The results for this comparative study are presented in Figure 14, and depict two distinct trends.

For double bottom, side shell and longitudinal bulkhead panels, not only the ratio between each TPPCA and bottom TPPCA remains asymptotically constant throughout the entire LPP scope, but it remains constant around the value of 1. On the other hand, for deck panels, the ratio between TPPCA and bottom TPPCA presents a linear behaviour, increasing with increasingly higher LPP values.

Regarding the production costs per unit area, the results shown in Figure 15 depict a slight decrease in the TPPCW with increase in LPP (as shown in the fitting line expression in Equation (21)).

$$TPPCW = -0.346 \times LPP + 849 \quad (21)$$

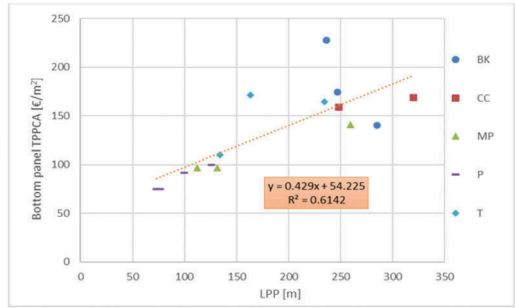


Figure 13. TPPCA [€/m²] as a function of LPP [m] for bottom panels.

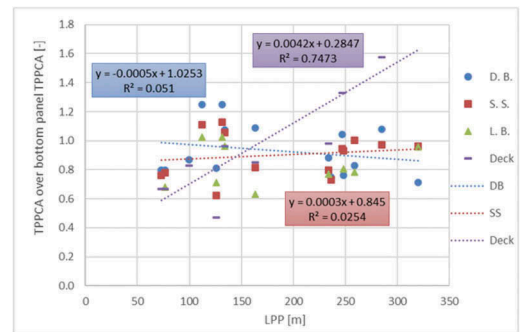


Figure 14. TPPCA over bottom TPPCA as a function of LPP [m].

Once again, a clear change on the overall TPPCW behaviour is observed at around LPP values of 200 m. The set of shorter vessels depicts a clear decrease in TPPCW with increasingly higher LPP values, while the set of longer vessels shows a constant TPPCW throughout the considered LPP range.

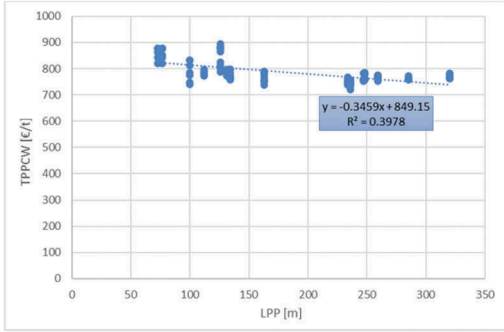


Figure 15. TPPCW [€/t] as a function of LPP [m].

It was also evaluated how the TPPCW of each panel type compares to the TPPCW of bottom panels. For this sake, the ratio between the TPPCW of each panel type and the TPPCW of the corresponding bottom panel (Equation (22)) is analysed as a function of LPP.

$$\frac{TPPCW_{chosen\ panel}^{ship\ n}}{TPPCW_{bottom\ panel}^{ship\ n}} \quad (22)$$

The TPPCW results for bottom panels presented in Figure 16 show a decrease on bottom TPPCW with the increase in LPP (this can be assessed using the shown overall fitting line expression).

The results shown in Figure 17 translate how for all the panel types considered in this study, the ratio between each TPPCW and bottom TPPCW remains asymptotically constant around the value of 1. This can be seen in the fitting line expression in Equation (23).

$$\frac{TPPCW}{TPPCW_{bottom}} = -0.0001 \times LPP + 1.05 \quad (23)$$

It is interesting to observe how such distinct types of panels present the same cost as the corresponding bottom panels, throughout the entire scope of considered LPP values.

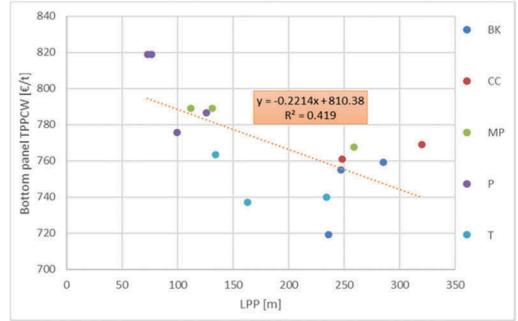


Figure 16. TPPCW [€/t] as a function of LPP [m] for bottom panels.

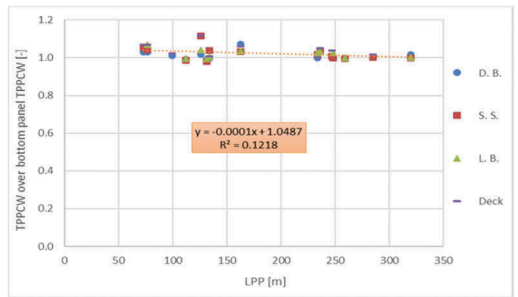


Figure 17. TPPCW over bottom TPPCW as a function of LPP [m].

5 CONCLUSIONS

The results obtained when assessing how stiffened panel strength was influenced by LPP showed a clear proportional increase in panel strength with increasingly higher LPP values. Both bottom and double bottom panel types presented a linear increase in panel strength up to LPP values around 200 m. For larger vessels, the panel strength would then reach an asymptotic value. The similarities between the results regarding these panel types are due to equal stiffener spacings and similar distances relatively to the midship section neutral axis.

When evaluating the influence of the panel aspect ratio, α , on the stiffened panel strength, most panel types presented a cluster-like behaviour. This means that most panel strength results were dispersed around a central α value, which seems somewhat optimal for the structure's integrity.

The local strength assessment led to two main conclusions: there's a general pattern of decrease in maximum bending stress over lateral pressure ratio with the increase in LPP and a visible increase in the pressure to reach bending yield stress with the increase in

LPP. Several panel types presented a more significant decrease in maximum bending stress for smaller vessels, stabilizing around a plateau for larger vessels. This behaviour is related to the difference between the structural approach at a global (stiffened panel strength) and local (local strength assessment) level. Concerning the influence of panel aspect ratio (α) on the local strength assessment, the results showed an overall tendency of increase in maximum bending stress over lateral pressure, with an increase in α and an overall tendency of decrease in the pressure to reach bending yield stress with increasingly higher α values.

Studies allowed to verify a clear linear increase in TPPCA with increasingly higher LPP values. For LPP values higher than 200 m, the TPPCA appeared to remain constant despite the increase in LPP. Besides, it was observed how for double bottom, side shell and longitudinal bulkhead panels the ratio between each TPPCA and respective bottom TPPCA remained asymptotically constant throughout the entire LPP scope (around 1). Regarding TPPCW, results showed a slight decrease with the increase in LPP. This result was of particular interest, as while results presented in terms of TPPCA showed that the profitability decreases for larger vessels, the TPPCW results depict an increase in profitability for larger vessels. When assessing the ratio between TPPCW for a given panel and TPPCW for the respective bottom panel, it was observed how this ratio remained around 1 throughout the entire LPP scope.

REFERENCES

- Adamchak, J.C. (1984). An approximate method for estimating the collapse of a ship's hull in preliminary design. *Proc. Ship Struct*, SNAME, 37–61.
- Billingsley, D.W. (1980). Hull girder response to extreme bending moments. *Proc. 5th STAR Symposium*, SNAME, pp. 51–64.
- Caldwell, J.B. (1965). Ultimate longitudinal strength. *Trans. RINA*, 107, 411–430.
- Columbus, L. (2018, August 8). Global State of Enterprise Analytics, 2018. *Forbes*.
- Faulkner, D. (1975). A review of effective plating for use in the analysis of stiffened plating in bending and compression. *Journal of Ship Research*, 19(1), 1–17.
- Faulkner, D., Adamchak, J. C., Snider, M. & Vetter, M. F. (1973). Synthesis of welded grillages to withstand compression and normal loads. *Computers and Structures*, 3, 221–246.
- Gordo, J. M., Carvalho, I. & Guedes Soares, C. (2006). Potencialidades de processos tecnológicos avançados de corte e união de aço em reparação naval. In *Inovação e Desenvolvimento nas Atividades Marítimas* (pp. 877–890). Edições Salamandra.
- Gordo, J. M. & Guedes Soares, C. (1993). Approximate load shortening curves for stiffened plates under uniaxial compression. In *Integrity of Offshore Structures—5* (pp. 189–211). EMAS.
- Leal, M. & Gordo, J. M. (2017). Hull's manufacturing cost structure. *Brodogradnja*, 68(3), 1–24. doi:10.21278/brod68301
- Lin, C.-K. & Shaw, H.-J. (2017). Feature-based estimation of preliminary costs in shipbuilding. *Ocean Engineering*, 144, 305–319.
- Lin, Y. T. (1985). *Ship longitudinal strength* [Ph.D. thesis]. University of Glasgow.
- Ljubenkov, B., Dukić, G. & Kuzmanić, M. (2008). Simulation Methods in Shipbuilding Process Design. *Journal of Mechanical Engineering*, 54, 131–139.
- Oliveira, A. & Gordo, J. M. (2018). Lean tools applied to a shipbuilding panel line assembling process. *Brodogradnja*, 69(4), 53–64. <https://doi.org/10.21278/brod6944>
- Rutherford, S. E. & Caldwell, J. B. (1990). Ultimate longitudinal strength of ships: A case study. *Trans. SNAME*, 98, 441–471.



Taylor & Francis

Taylor & Francis Group

<http://taylorandfrancis.com>